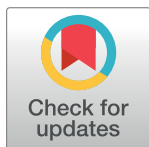# PLOS ONE

RESEARCH ARTICLE

Identification of cell lines CL-14, CL-40 and CAL-51 as suitable models for SARS-CoV-2 infection studies

Claudia Pommerenke[1☯*], Ulfert Rand[2☯], Cord C. Uphoff[3☯], Stefan Nagel[3], Margarete Zaborski[3], Vivien Hauer[3], Maren Kaufmann[3], Corinna Meyer[3], Sabine A. Denkmann[3], Peggy Riese[2], Kathrin Eschke[2], Yeonsu Kim[2], Zeljka Macak Safranko[4], Ivan-Christian Kurolt[4], Alemka Markotic[4], Luka Cicin-Sain[2,5], Laura Steenpass[3]

1 Department of Bioinformatics and Databases, Leibniz Institute DSMZ - German Collection of Microorganisms and Cell Cultures, Braunschweig, Germany, 2 Department of Vaccinology and Applied Microbiology, Helmholtz Centre for Infection Research, Braunschweig, Germany, 3 Department of Human and Animal Cell Lines, Leibniz Institute DSMZ - German Collection of Microorganisms and Cell Cultures, Braunschweig, Germany, 4 Dr. Fran Mihaljević University Hospital for Infectious Diseases, Zagreb, Croatia, 5 Centre for Individualized Infection Medicine, a Joint Venture of Helmholtz Centre for Infection Research and Medical School Hannover, Hannover, Germany

☯ These authors contributed equally to this work.
* claudia.pommerenke@dsmz.de

Abstract

The SARS-CoV-2 pandemic is a major global threat that sparked global research efforts. Pre-clinical and biochemical SARS-CoV-2 studies firstly rely on cell culture experiments where the importance of choosing an appropriate cell culture model is often underestimated. We here present a bottom-up approach to identify suitable permissive cancer cell lines for drug screening and virus research. Human cancer cell lines were screened for the SARS-CoV-2 cellular entry factors *ACE2* and *TMPRSS2* based on RNA-seq data of the Cancer Cell Line Encyclopedia (CCLE). However, experimentally testing permissiveness towards SARS-CoV-2 infection, we found limited correlation between receptor expression and permissiveness. This underlines that permissiveness of cells towards viral infection is determined not only by the presence of entry receptors but is defined by the availability of cellular resources, intrinsic immunity, and apoptosis. Aside from established cell culture infection models CACO-2 and CALU-3, three highly permissive human cell lines, colon cancer cell lines CL-14 and CL-40 and the breast cancer cell line CAL-51 and several low permissive cell lines were identified. Cell lines were characterised in more detail offering a broader choice of non-overexpression in vitro infection models to the scientific community. For some cell lines a truncated *ACE2* mRNA and missense variants in *TMPRSS2* might hint at disturbed host susceptibility towards viral entry.

Introduction

It is of no debate that the overcoming of the pandemic SARS-CoV-2 pathogen spreading across the continents urgently needs joint efforts in the scientific community. Within a few months in the midst of spring 2020 the pandemic was accompanied with a high case fatality rate of up to 20% for vulnerable risk groups [1] and high excess mortality in Europe monitored by EuroMOMO (https://www.euromomo.eu/graphs-and-maps) [2]. High transmissibility of SARS-CoV-2 with R0 of ∼ 2.5 exceeds that of SARS-CoV, the 2009 influenza A H1N1 virus and even the 1918 influenza pandemic [3], probably due to its airborne transmission via droplets and aerosol [4–6]. During summer time, the portion of asymptomatic cases in a small Italian village were quantified to 43% [7] and since pre-/asymptomatic virus carriers were observed to be contagious, these are thought to drive the pandemic [8]. Re-infection also has been reported to complicate the pandemic course [9].

While various vaccines are rolled out [10–12], options for antiviral treatment for severely diseased patients are still sparse. Neutralising antibodies are promising drugs [13], while small molecules like remdesivir [14] have not yet proven great benefits [15, 16]. Importantly, all future antivirals, when becoming available and broadly used, face the challenge of SARS-CoV-2 escape mutations [17, 18]. Thus, it is clear that drug screening and basic research in SARS-CoV-2 is and will be of continuous importance.

Current investigations are mainly limited to the VERO-E6 African green monkey cell line, human lung cancer-derived CALU-3 and human colon carcinoma cell line CACO-2. Using non-human cells to study SARS-CoV-2 bears the inherent risk to draw conclusions from findings that result from species-specific cell properties. The anti-SARS-CoV-2 properties of hydroxychloroquine were found using VERO-E6, while later studies detected no effect in human cells and patients [19, 20]. In addition, the virus mutates rapidly when replicating in VERO-E6 [21–23]. Overexpression of host factors, such as TMPRSS2, can overcome individual species-specific artefacts but comes with commonly observed difficulties of stable transgene expression, such as antibiotic selection, non-physiological protein level, or transgene silencing during passaging.

Human cancer cell lines are easily available from public collections, characterised in great detail, and offer a great range of tissue origins, expression patterns, growth rates, and functional properties to choose from. They serve as valuable and valid model systems to study different diseases [24, 25] and have been used specifically for SARS-CoV-2 viral entry [26, 27] or for antiviral studies against this virus [28]. Particularly the two surface proteins ACE2 and TMPRSS2 have been shown to contribute to viral binding and processing [26, 27] and are mainly expressed in bronchial transient secretory cells [29]. Interestingly, high gene expression of *ACE2* is shown for other tissues such as myocardial cells, esophagus epithelial cells, and enterocytes, which might be related to non-respiratory symptoms observed in COVID-19 patients [30–33]. Many virus-host-interaction studies rely on *ACE2/TMPRSS2*-transfected cell lines such as 293T and HELA cells or non-human material such as African green monkey cells VERO-E6 [26, 34, 35]. A recent study validated HPAEpiC as a human AT2 cell-derived pulmonary alveolar epithelial cell line to be susceptible to SARS-CoV-2 [36].

In this study, we have pre-screened and ranked human cancer cell lines of the Leibniz Institute German Collection of Microorganisms and Cell Cultures (DSMZ) for *ACE2* and *TMPRSS2* expression within the rich resource Cancer Cell Line Encyclopedia (CCLE) publicly available RNA-seq data [37]. Selected cell lines were then validated for mRNA and protein levels of ACE2 and TMPRSS2 and tested in SARS-CoV-2 infection experiments, revealing a set of cell lines displaying high and low permissiveness. With these cell lines we devise appropriate,

non-overexpressing cell model systems to facilitate experimental SARS-CoV-2 work for the understanding of viral entry, viral replication and to support drug development.

Results

Selection of cell model systems

Inspired by the publication of Hoffmann et al. pinpointing the host factors ACE2 as SARS-CoV-2 receptor and TMPRSS2 as viral S protein priming serine protease [26], we defined expression of these two factors as pre-selection criteria in our study. Since the Cancer Cell Line Encyclopedia (CCLE) as a comprehensive database provides large-scale sequencing data including mRNA-seq expression data for over 900 cell lines [37], we screened for gene expression of *ACE2* and *TMPRSS2* in this data set, which enabled us to identify potential susceptible cell lines prone to SARS-CoV-2 virus entry. At first, we selected for 301 human cell lines readily in stock at the DSMZ cell lines repository within this data set and visualised gene expression of *ACE2*, which was shown to be the cellular receptor for the viral S protein [38], and *TMPRSS2* known to cleave SARS-CoV S protein [39] (Fig 1A). Gene expression for these two genes differed between and within the various tumour entities. In order to pre-select cell lines to be tested for SARS-CoV-2 permissiveness, the top 25 highest *ACE2* gene expressing cell lines were selected, originating from diverse tumour origins (Fig 1B). Importantly, our short-list included cancer cell lines originating from tissues that are known for SARS-CoV-2 replication in vivo [40], e.g. the tongue squamous cell carcinoma cell lines CAL-27, CAL-33, and the esophageal squamous cell carcinoma cell line KYSE-510. Based on this evidence, we additionally selected the newly established oral squamous cell carcinoma cell lines UPCI-SCC-074 and UPCI-SCC-131, which are not contained in the CCLE dataset. Futhermore, we included the neuronal cells DBTRG-05MG and KELLY with high levels of neuropilin 1 (*NRP1*) mRNA expression (Fig 1B), which has been discussed as receptor for the viral spike protein [41, 42]. *NRP1* expression was most prominent in DBTRG-06MG, CAL-51, CAL-85–1, CALU-3, SCC-25, CL-40, and KELLY (Fig 1B). Since the lung carcinoma cell line CALU-3, the colorectal adenocarcinoma CACO-2, and the green monkey kidney cell line subclones VERO-E6 and
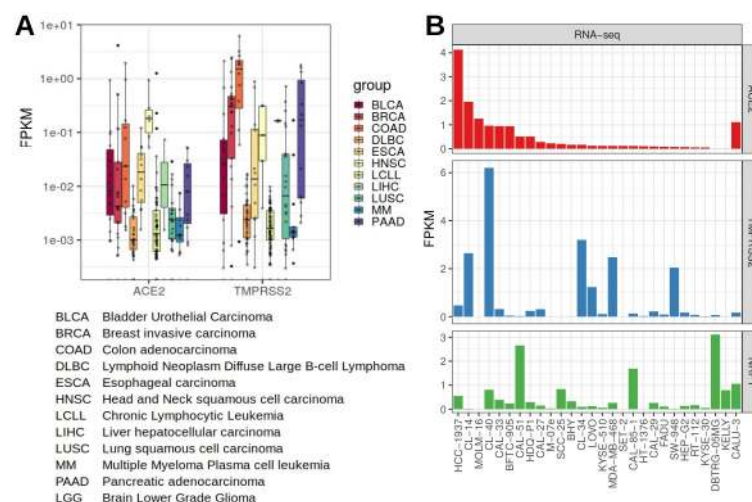

BLCA Bladder Urothelial Carcinoma
BRCA Breast invasive carcinoma
COAD Colon adenocarcinoma
DLBC Lymphoid Neoplasm Diffuse Large B-cell Lymphoma
ESCA Esophageal carcinoma
HNSC Head and Neck squamous cell carcinoma
LCLL Chronic Lymphocytic Leukemia
LIHC Liver hepatocellular carcinoma
LUSC Lung squamous cell carcinoma
MM   Multiple Myeloma Plasma cell leukemia
PAAD Pancreatic adenocarcinoma
LGG   Brain Lower Grade Glioma

Fig 1. *ACE2* and *TMPRSS2* gene expression data for 301 DSMZ human cell lines in the CCLE RNA-seq data set. A: Expression of *ACE2* and *TMPRSS2* for selected disease entities. RNA-seq data were normalised and calculated to FPKM values. Gene expression for *ACE2* and *TMPRSS2* varies between and within the different tumour species. B: Expression of *ACE2*, *TMPRSS2* and *NRP1*, cell lines sorted to *ACE2* expression levels. Top 25 *ACE2* expressing cell lines were selected for further studies, plus CALU-3 and two further neuronal cell lines with high *NRP1* levels. FPKM—fragments per kilobase million: normalised gene expression data.
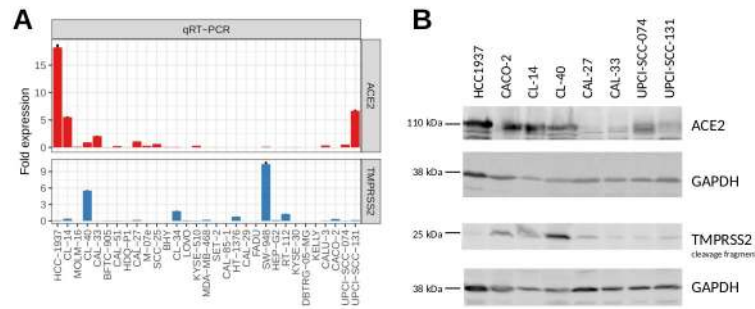
Fig 2. Verified presence of ACE2 and TMPRSS2 in carcinoma cell lines determined by qRT-PCR and western blots. A: Quantification of *ACE2* and *TMPRSS2* transcripts in the selected candidate cell lines by qRT-PCR (normalised to CAL-27 and CL-40). B: Western blot analysis was performed to assess the expression of proteins associated with SARS-CoV-2 cell entry.

https://doi.org/10.1371/journal.pone.0255622.g002

VERO-B4 are shown to be permissive for SARS-CoV-2 [26, 27], these were used as positive control cell lines. Altogether we selected 29 human cancer cell lines and four control cell lines.

In order to validate *ACE2* and *TMPRSS2* expression levels, we performed qRT-PCR on the short-listed cell lines. All selected cell lines exhibited considerable *ACE2* mRNA expression according to the RNA-seq data and/or qRT-PCR except for DBTRG-05MG and KELLY, whereas *TMPRSS2* mRNA levels were particularly higher in CL-40, CL-34, CL-14, and SW-948 (Figs 1B and 2A). Apart from qualitative verification for mRNA expression via RNA-seq data and qRT-PCR (Fig 2A), protein expression of ACE2 and TMPRSS2 was confirmed via western blot for specific cell lines (Fig 2B, S1 Fig).

For expanding our cell line search spectrum, we interrogated the LL-100 cell line data set, comprising RNA-seq and whole-exome sequencing (WES) data of 100 human leukemia and lymphoma cell lines [24]. However, none of these cell lines showed considerable expression of *ACE2* and *TMPRSS2*. This is reflected in the CCLE results, in which cell lines of the hemato-poetic lineages exhibited lower gene expression of both genes compared to other cell lines of different origin (see Fig 1A DLBC, LCLL and MM tumour entities).

The presence of the entry factors ACE2 and TMPRSS2 in cancer cell lines of various origins is in accordance with their expression in corresponding primary tissue, where *ACE2* and *TMPRSS2* were detected in cells from multiple tissues including respiratory tract, esophagus and colon [31, 33, 43–45] and virus entry was evidenced in gastro-intestinal tissues [46], organs of the respiratory tract and various other tissues [40].

Testing for SARS-CoV-2 infectivity and permissiveness

Receptor ACE2 and surface proteinase TMPRSS2 have been shown to play a key role for SARS-CoV-2 cellular entry, however, whether their co-expression is sufficient to allow entry and whether alternative receptors may exist, is still under debate [45]. In order to shed light on infectivity and permissiveness of the appointed cell lines in context of their ACE2/TMPRSS2 expression, we subjected cells to experimental infection with wildtype SARS-CoV-2. Permissiveness to viral infection is defined as the ability of a given host cell to permit the entire viral replication cycle and to eventually release mature virions. Thus, we sampled the supernatant of the short-listed cell lines at four consecutive days following infection with a low amount of inoculum to sensitively detect viral replication.

Within our short-listed panel, we identified large variation in the degree of permissiveness and virus replication kinetics. Surprisingly, the majority of tested cell lines (15 of 29) showed no detectable virus replication despite the presence of ACE2 and TMPRSS2 (Fig 3A, S2 Fig).
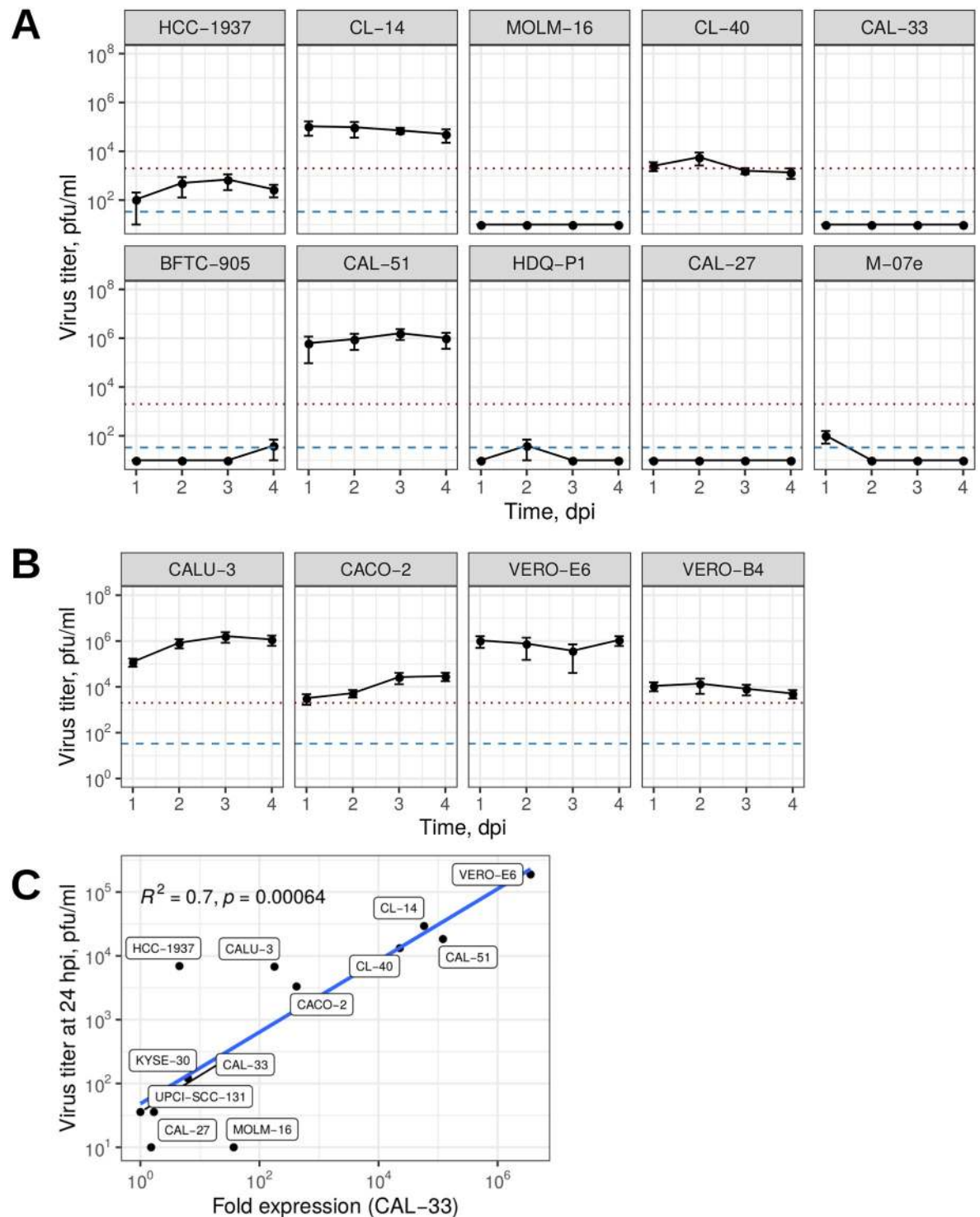
Fig 3. Susceptibility of tumour cell lines toward SARS-CoV-2 infection. Virus titers in the supernatant of infected cell lines at 1–4 days postinfection (dpi) determined by plaque assay for the top 10 ACE2 expressing cell lines (A) and controls (B). The red dotted line indicates the initial inoculum (2000 pfu/ml); the blue dashed line specifies the minimal limit of detection LOD 33.3 pfu/ml. Number of replicates varied between 3–8. pfu: plaque-forming units; mean values with SEM. (C) Predominant productive virus production in highly permissive cell lines seen in the correlation between qRT-PCR measured viral nucleoprotein N mRNA and releasing virions tested by viral plaques. Eight replicates served for the means of the viral titers and one representative expression fold change of two biological replicates qRT-PCR with three technical replicates. Note the logarithmic scaling for both x and y-axis.

https://doi.org/10.1371/journal.pone.0255622.g003

Table 1. Permissive cell line characteristics.

cell line	Species	Sex	Tissue	Peak viral load, dpi	Maximal peak, pfu/ml	Doubling time
CL-14	human	male	colon	1	1.1×10^5	$\sim$ 1w
CL-40	human	female	colon	2	5.8×10^3	$\sim$ 3–4d
CAL-51	human	female	breast	3	1.6×10^6	$\sim$ 30h*
CALU-3	human	male	lung	3	1.6×10^6	$\sim$ 84h*
CACO-2	human	male	colon	4	3.0×10^5	80h
VERO-B4	monkey	female	kidney	2	1.4×10^5	$\sim$ 25h
VERO-E6	monkey	female	kidney	4	1.1×10^6	22h[+]

Peak viral load and maximal peak were determined during this study.

Species, sex, tissue and doubling time were taken from https://www.dsmz.de/collection/catalogue/human-and-animal-cell-lines/catalogue.

*own observation;

[+]ATCC.

https://doi.org/10.1371/journal.pone.0255622.t001

Further 11 cell lines showed detectable SARS-CoV-2 infectious titres that did not exceed the amount of the inoculum. Only three cell lines were categorized highly permissive, amplifying the initial virus inoculum by factors of $\sim$ 2 to $\sim$ 500 between 1 and 4 dpi. These were the colon carcinoma cell lines CL-14 and CL-40, as well as breast carcinoma cell line CAL-51. Infectious titres of SARS-CoV-2 grown on CL-14 and on CAL-51 were concurrent with the widely used CALU-3 (lung carcinoma), CACO-2 (colon carcinoma), VERO-E6 and VERO-B4 (normal African green monkey kidney cells) (Fig 3B). Whereas CL-14 already has been described to be permissive in a preprint [47], the breast carcinoma cell line CAL-51 with high levels of *NRP1* beside *ACE2* and *TMPRSS2* expression and the colon carcinoma cell line CL-40 have not been identified before. Despite comparable peak titres, virus replication kinetics differed largely between cell lines, where CAL-51 and CACO-2 showed increase in titres throughout day three postinfection while VERO-E6, VERO-B4, and CL-14 produced highest levels within 24h, while the viral titer for CL-40 remained close to the level of the initial inoculum of SARS-CoV-2 (Fig 3, Table 1).

Therapeutic neutralising antibodies bind to the viral Spike protein and prevent the interaction with ACE2 [13]. However, it is unclear whether different levels of ACE2 expression on the surface of cells would interfere with the ability to block virus entry. Thus, we used three different permissive cell lines of our panel (CL-14, CAL-51, and VERO-E6) with varying ACE2 levels and performed in vitro neutralisation assays using the therapeutic anti-Spike antibody COR-101 currently used in clinical trials (see S3 Fig) [48]. While the comparability among these cell lines is limited due to several variables (cell density, virus growth kinetic, cell medium, etc.), we observed ≥93% inhibition of virus entry at 100 ng/ml in all three cell lines, compared to the lowest nAb concentration. The inhibition curves suggest a reduced neutralisation efficiency in the CAL-51 breast cancer cell line, which might be attributed to NRP-1-mediated or NRP-1-assisted virus entry [41, 42]. NRP-1 is an alternative or assisting SARS-CoV-2 entry factor that shows elevated levels in CAL-51 cells (see Fig 1A). However, the complete virus neutralisation at sufficient antibody levels suggests either the absence of ACE2-independent entry or the additional inhibition of a Spike/NRP-1 interaction.

In contrast, low-permissive cell lines, such as the breast cancer HCC-1937, the colon adenocarcinoma CL-34, and esophageal squamous cell carcinoma KYSE-30 cell lines showed slow replication kinetics, which was also true for the oral squamous cell carcinoma cell lines UPCI-SCC-074 and UPCI-SCC-131 but not for the neuronal cells DBTRG-05MG and KELLY

despite high levels of *NRP1* ([Fig 3A](#), [S2 Fig](#)). Non-permissive cell lines showed no detectable SARS-CoV-2 titres at any time after infection.

In order to test for abortive viral cycles particularly in the non-productive virus releasing cell lines, we compared mRNA levels of the nucleoprotein in each three control, high-permissive, low-permissive, and non-permissive cell lines to viral plaques after 24 hpi ([Fig 3C](#)). We found a high correlation ($R^2 = 0.7$) between viral expression and infective virus titers in the tested cell lines, probably reduced by high variation in viral infection of the cell lines at detection limit. Hence, these data argue for the absence of abortive virus replication or defects in releasing mature virions in the low-permissive cell lines.

Genomic analyses of *ACE2* and *TMPRSS2*

Since we found limited concordance between *ACE2/TMPRSS2* expression and virus permissiveness of the cell lines, we seeked for genomic differences in the receptors. Of note, gene expression of different splice variants of the *ACE2* mRNA became evident comparing the read numbers of the exons as seen in the CCLE RNA-seq data for MOLM-16, CAL-33, BFTC-905, and CAL-27 ([Fig 4A](#), [S4 Fig](#), [S1 Table](#)). The truncated *ACE2* lacking exon 1–9 has been reported recently [49, 50].

Furthermore, missense variants were detected in *TMPRSS2* for HCC-1937 (homozygous), CL-40 (heterozygous), CAL-33 (homozygous), and HDQ-P1 (heterozygous) ([Fig 4B](#)), namely V197M (V160M) in exon 6 (rs12329760) and/or G8V in exon 1 (rs75603675). We assume that these variations may have a considerable effect on the virus-host interaction.
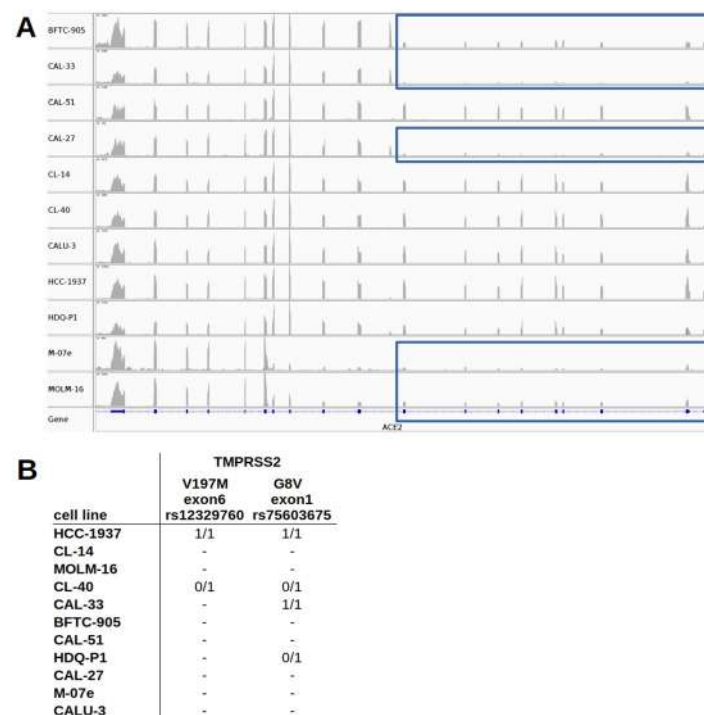

cell line	V197M exon6 rs12329760	G8V exon1 rs75603675
HCC-1937	1/1	1/1
CL-14	-	-
MOLM-16	-	-
CL-40	0/1	0/1
CAL-33	-	1/1
BFTC-905	-	-
CAL-51	-	-
HDQ-P1	-	0/1
CAL-27	-	-
M-07e	-	-
CALU-3	-	-

Fig 4. *ACE2* and *TMPRSS2* transcript variants for the cell lines. A: Different exon usage of *ACE2* for the top 10 *ACE2* expressing cell lines plus CALU-3 (see [S2 Fig](#) for the top 25 cells). BFTC-905, CAL-33, CAL-27, M-07e, and MOLM-16 show reduced exon expression from exon 1–9 (blue rectangles). Cell lines are ordered alphabetically. *ACE2* is reversely oriented. B: Missense variants in the coding regions of *TMPRSS2* (V197M = rs12329760, G6V = rs75603675) for the selected cell lines. No mutations were found in the coding regions of *ACE2*. 0/1 denotes heterozygous and 1/1 homozygous mutations.

https://doi.org/10.1371/journal.pone.0255622.g004

Discussion

In this study, we have systematically identified and characterised SARS-CoV-2 permissive cancer cell lines that (except one) have not been published as such before. Of 29 selected human cell lines three tested high-level positive permissive for SARS-CoV-2. These selected cell lines are available from the German repository DSMZ. Cancer cell lines have been an integral tool for basic research and drug screening for decades and still are the preferred choice for the vast majority of virus research labs. For SARS-CoV-2 infection experiments, different replication kinetics as well as different degrees of permissiveness can aid answering specific questions and allow different experimental setups, e.g. in compound screening assays. We found permissiveness to SARS-CoV-2 in only 14 out of 29 cell lines pre-selected for the expression of the known entry factor *ACE2* (Figs 1B and 2). Three of them replicated the virus to high titres (CL-14, CL-40, and CAL-51) and further 11 showed low levels with mainly slow virus kinetics compared to commonly used VERO-E6, CALU-3, and CACO-2 cells (Fig 3, S2 Fig, Table 1).

In order to understand the non-permissiveness of the majority of top 25 *ACE2* expressing cell lines, we closely examined splice and single nucleotide variants. *ACE2* splice variants at the N-terminus, containing eight amino acids critical for binding to the receptor binding domain (RBD) of the spike protein of SARS-CoV-2, are predicted to disturb SARS-CoV-2 attachment [51]. One splice variant lacking exon1-exon9 was observed in e.g. MOLM-16, CAL-33, and CAL-27 (Fig 4A, S4 Fig, S1 Table), cell lines that indeed were not shown to be non-permissive despite their pronounced *ACE2* gene expression (Fig 1B). This truncated *ACE2* isoform has been reported to be interferon inducible [49] and fails to bind to SARS-CoV-2 [50].

Whereas the lacking permissiveness for SARS-CoV-2 of the above mentioned cell lines is likely to be explained by a truncated *ACE2* transcript (Fig 4A), it is more challenging to elucidate, why the candidate cell line CL-40 tested less permissive than CL-14 and CAL-51 despite high *TMPRSS2* transcript levels. CL-40 as well as HCC-1937 hold a missense variation in exon 6 of TMRPSS2 (Fig 4B) causing an amino acid exchange at position 197 (V197M/V160M) within the Scavenger receptor cysteine-rich (SRCR) domain responsible for protein-protein interaction and ligand binding (ExPASy) and is described for various cancer types as well as cell lines (COSMIC). Hence, we speculate that interaction with SARS-CoV-2 might be disturbed by this variant at V197M, which is known for differential allelic frequencies in populations [52].

Importantly, the expression levels of *ACE2*, *TMPRSS2* and *NRP1* are not predictive of SARS-CoV-2 permissiveness per se. While *ACE2* seems to be an essential component, however, it is not sufficient on its own. Permissiveness includes the ability of the virus to enter the cell, replicate, and release infectious progeny. A number of cellular processes can effectively interfere with this replication cycle, including intrinsic immune response, type-I and type-III interferon responses and apoptosis induction [53] and thus determine permissiveness. For SARS-CoV-2, several essential host factors apart from surface receptors were recently discovered [54].

Meanwhile, several organs and cell types have been reported to be infected by SARS-CoV-2, even for those with no or low basal *ACE2* expression [30, 45]. Hence, alternate receptors, proteases and antagonists for SARS-CoV-2 infection could widen the options for viral entry [45] as shown for cathepsin L [55] and CD147 [56]. Besides genetic and epigenetic variations, variable activation of ACE2 could also be triggered by interferon pathways [57, 58].

Seeking for SARS-CoV-2 permissive cell lines by screening *ACE2* RNA-seq-derived expression levels, the human native breast carcinoma cell line CAL-51 and the colon adenocarcinoma cell lines CL-40 and CL-14 have been identified to produce high levels of infectious SARS-CoV-2 virus particles. CAL-51 in particular could enrich SARS-CoV-2 studies trifold:

low doubling time of this cell line, viral stock production comparable to commonly used VERO-E6, and a further organ tissue as infection model. Its doubling time is lower than that of the colon carcinoma cell lines CACO-2/CL-14 and the lung carcinoma cell line CALU-3 (Table 1), avoiding the mutation selection pressure to adapt to another species host as seen for the African green monkey cell line VERO-E6 [21–23]. Different replication kinetics as well as different degrees of permissiveness can aid answering specific scientific questions and allow different experimental setups, e.g. in compound screening assays.

In summary, we find that the expression of *ACE2* and *TMPRSS2* are indicative but not sufficient for SARS-CoV-2 productive infection in human cell lines, probably partly due to a truncated *ACE2* splice variant and *TMPRSS2* variants. Out of 29 tested cancer cell lines, we have identified three highly and 11 lowly permissive cell lines that vastly broaden the choice for SARS-CoV-2 cell culture models. The breast carcinoma cell line CAL-51 in particular may serve as a suitable cell line for SARS-CoV-2 studies for viral propagation because of its easy management.

Methods

CCLE RNA-seq data set analysis

RNA-seq data were retrieved and pre-processed as described [59]. Briefly, alignment files were downloaded from CGHub via genetorrent, sorted (samtools 0.1.19) and converted to fastq files (bedtools v2.21.0). Reads were trimmed via fastq-mcf (ea-utils 1.1.2–686). STAR (2.5.3a) served as read mapper to the human genome Gencode 26, HTSeq (0.11.3) was used as count tool. Raw counts were normalised and transformed to FPKM (fragments per kilobase million) via R/Bioconductor (3.6.9) loading DESeq2 (1.26.0) and visualised via ggplot2 (3.1.1). Different exon usage was discovered by visualising the alignment files via IGV (2.8.0) [60]. For detecting mutations, mapped reads were assigned to read groups (picard, 2.9.2 [www.broadinstitute.github.io/picard]); reads were split, trimmed and reassigned (GenomeAnalysisTK, 3.7–0, SplitNCigarReads [61]); mutations were called by the HaplotypeCaller (GenomeAnalysisTK, 3.7–0,) [61]; and mutation effects were predicted via the Ensembl VEP (GRCh38, v90) [62]. Mutations were filtered to ≥10 depth.

Cultivation of human cell lines

The continuous cell lines are part of the cell culture collection at DSMZ (https://www.dsmz.de/collection/catalogue/human-and-animal-cell-lines). Tissue origin, doubling-time, growth properties, cytogenetics and more information on these cell lines can be retrieved from the DSMZ website. Cell lines were grown at 37˚C in a humidified atmosphere of air containing 5% CO_2. The basic growth media (Life Technologies, Darmstadt, Germany) were supplemented with 10–20% fetal bovine serum (Sigma Aldrich, Taufkirchen, Germany). No antibiotics were added to the cultures. All cell lines were free of mycoplasma and other bacterial, yeast and fungi contaminations as tested by PCR and microbiological growth assays [63]. The authenticity of the cell lines was determined by DNA typing [64]. The cells were first cultured in cell culture flasks to confluence, detached with trypsin/EDTA, washed with PBS and pelleted for RNA and protein preparation. For virus infection experiments the cells were seeded in 96-well plates at different densities starting with 0.25—1.5 x 105 cells per well as highest cell number depending on the cell line. Optimal cell densities were determined by observing the growth progression with an IncuCyte instrument (Essen Bioscience, Hertfordshire, UK). Cells were then seeded at semi-confluence or complete confluence and three further dilutions each with half of the previous cell densities. The cells were grown for one day before the virus infection experiments were started.

qRT-PCR analysis

Quantitative Real-time polymerase chain reaction (qRT-PCR) analysis for human mRNA was performed to quantify specific transcripts in the cells. Total RNA was extracted from cell line samples using TRIzol reagent (Fisher Scientific, Schwerte, Germany). cDNA was generated from 1 µg RNA by random priming using the Biozym cDNA Synthesis Kit (Biozym, Hessisch Oldendorf, Germany). qRT-PCR analysis was performed with the 7500 Real-time System, using commercial buffer and primer sets for the amplification of *ACE2* (Hs01085333_m1) and *TMPRSS2* (Hs01122322_m1) transcripts (Thermo Fisher Scientific, Darmstadt, Germany).

Viral RNA of infected cell cultures was extracted using spin filter membranes (innuPREP Virus TS RNA Kit from Analytik Jena) according to the manufacturer's recommendations. Briefly, cells were lysed in the presence of carrier RNA and Proteinase K at 70˚C for 10 min. Nucleic acids were then bound to the surface of the spin filter membranes, washed and subsequently eluted with RNase-free water. One to five μg RNA were then reverse transcribed to cDNA applying random hexamers. The primers for the qRT-PCR for the amplification of the SARS-CoV-2 N gene were N_Sarbeco_F (5´-CACATTGGCACCCGCAATC-3') and N_Sarbeco_R (5'-GAGGAACGAGAAGAGGCTTG-3') [65].

We analysed the transcript of TATA box binding protein (TBP) for normalisation of expression levels using SYBR Green for quantification. Quantitative analyses were performed in triplicate, if not indicated differently, analysed and visualised with R/Bioconductor packages ddCt and ggplot2.

Western blots

Antibodies against ACE2 (ab15348), TMPRSS2 (ab109131), and GAPDH (ab8245) were obtained from Abcam (Cambridge, UK). Western blot samples were prepared as described previously [66]. Proteins on nitrocellulose membranes were visualized with the biotin/strepta-vidin-horseradish peroxidase system (GE Healthcare; Little Chalfont, UK) in combination with the "Renaissance Western Blot Chemoluminescence Reagent" (Perkin Elmer; Waltham, MA, USA). Documentation was performed using the digital system ChemoStar Imager (INTAS, Göttingen, Germany).

Viral infection of cell lines

Infection with SARS-CoV-2 was performed with virus strain Zagreb (SARS-CoV2/ZG/297–20, University Hospital for Infectious Diseases, Zagreb, Croatia). If not indicated otherwise, cells were seeded onto 96-well cell culture plates and infected 24–48 hours later with 250 pfu/well using a 10 μl inoculum and 100 μl total well volume.

Virus plaque and neutralisation assays

Quantification of SARS-CoV-2 infectious units was done via a virus plaque assay. Supernatants of infected cells were taken 1–4 dpi, serially diluted, and used to infect confluent VERO-E6 cells on 96-well cell culture plates for one hour. Then, the inoculum was removed and cells were overlaid with cell culture medium (MEM, 10% FCS, 2 mM glutamine) containing 1.5% methyl-cellulose. After 3 days, virus plaques were counted from phase contrast microscopic images taken with a Sartorius IncuCyte S3 at 4x magnification.

For neutralisation assays antibody COR-101 and virus were mixed and incubated for 1h at 37˚C and applied to cells for 24 hpi. COR-101 for was a kind gift of Corat Therapeutics GmbH (Braunschweig, Germany).

Supporting information

S1 Fig. Original western blots. Original western blots to cropped western blot images in Fig 2B.
(PDF)

S2 Fig. Virus titers. Virus titers in the supernatant of infected cell lines at 1-4 dpi determined by plaque assay for the top 11-25 *ACE2* expressing, two neuronal (DBTRG-05MG, KELLY), and two oral squamous cell carcinoma (UPCI-SCC-074, UPCI-SCC-131) cell lines. The red dotted line indicates the initial inoculum (2000 pfu/ml); the blue dashed line specifies the minimal limit of detection LOD 33.3 pfu/ml. Number of replicates varied between 3-8. pfu: plaque-forming units; mean values with SEM.
(TIFF)

S3 Fig. Neutralisation assays. Neutralising SARS-CoV-2 antibody was applied to the high permissive cell lines CAL-51 and CL-14 and the control cell line VERO-E6. With increasing antibody concentration viral production is decreasing in all three cell lines. The red dotted line indicates the initial inoculum (2000 pfu/ml); the blue dashed line specifies the minimal limit of detection LOD 33.3 pfu/ml. Note the logarithmic scaling for the x-axis.
(TIF)

S4 Fig. *ACE2* splicing variant. Different exon usage of *ACE2* for the top 25 *ACE2* expressing cell lines plus CALU-3. RNA-seq data were visualised via IGV and cell lines ordered alphabetically.
(TIFF)

S1 Table. Summary cell lines. Gene expression, splice and single nucleotide variants of *ACE2* and *TMPRSS2* in the cell lines used in this study. These were identified on the basis of CCLE RNA-seq data (FPKM, see Material and methods). +truncated splice variant observed; 0/1 heterozygous, 1/1 homozygous mutation.
(ODS)

Acknowledgments

Author Contributions

Conceptualization: Claudia Pommerenke, Ulfert Rand, Cord C. Uphoff, Laura Steenpass.

Formal analysis: Claudia Pommerenke, Ulfert Rand, Cord C. Uphoff, Stefan Nagel.

Investigation: Claudia Pommerenke, Ulfert Rand, Stefan Nagel, Margarete Zaborski, Vivien Hauer, Maren Kaufmann, Corinna Meyer, Sabine A. Denkmann, Peggy Riese, Kathrin Eschke, Yeonsu Kim.

Methodology: Claudia Pommerenke, Ulfert Rand, Cord C. Uphoff.

Project administration: Claudia Pommerenke, Cord C. Uphoff.

Resources: Zeljka Macak Safranko, Ivan-Christian Kurolt, Alemka Markotic.

Supervision: Claudia Pommerenke, Ulfert Rand, Cord C. Uphoff, Luka Cicin-Sain, Laura Steenpass.

Visualization: Claudia Pommerenke.

Writing – original draft: Claudia Pommerenke, Ulfert Rand.

Writing – review & editing: Claudia Pommerenke, Ulfert Rand, Cord C. Uphoff, Laura Steenpass.

References

1. Onder G, Rezza G, Brusaferro S. Case-fatality rate and characteristics of patients dying in relation to COVID-19 in Italy. JAMA. 2020; 323(18):1775–1776. PMID: 32203977

2. Kanieff M, Rago G, Minelli G, Lamagni T, Sadicova O, Selb J, et al. The potential for a concerted system for the rapid monitoring of excess mortality throughout Europe. Euro Surveill. 2010; 15(43):19697. https://doi.org/10.2807/ese.15.43.19697-en PMID: 21087579

3. Petersen E, Koopmans M, Go U, Hamer DH, Petrosillo N, Castelli F, et al. Comparing SARS-CoV-2 with SARS-CoV and influenza pandemics. Lancet Infect Dis. 2020; 20(9):e238–e244. https://doi.org/10.1016/S1473-3099(20)30484-9 PMID: 32628905

4. van Doremalen N, Bushmaker T, Morris DH, Holbrook MG, Gamble A, Williamson BN, et al. Aerosol and Surface Stability of SARS-CoV-2 as Compared with SARS-CoV-1. N Engl J Med. 2020; 382 (16):1564–1567. https://doi.org/10.1056/NEJMc2004973 PMID: 32182409

5. Tang S, Mao Y, Jones RM, Tan Q, Ji JS, Li N, et al. Aerosol transmission of SARS-CoV-2? Evidence, prevention and control. Environ Int. 2020; 144:106039. https://doi.org/10.1016/j.envint.2020.106039 PMID: 32822927

6. Fears AC, Klimstra WB, Duprex P, Hartman A, Weaver SC, Plante KS, et al. Persistence of Severe Acute Respiratory Syndrome Coronavirus 2 in Aerosol Suspensions. Emerg Infect Dis. 2020; 26 (9):2168–2171. https://doi.org/10.3201/eid2609.201806

7. Lavezzo E, Franchin E, Ciavarella C, Cuomo-Dannenburg G, Barzon L, Del Vecchio C, et al. Suppression of a SARS-CoV-2 outbreak in the Italian municipality of Vo'. Nature. 2020; 584(7821):425–429. https://doi.org/10.1038/s41586-020-2488-1 PMID: 32604404

8. Nikolai LA, Meyer CG, Kremsner PG, Velavan TP. Asymptomatic SARS Coronavirus 2 infection: Invisible yet invincible. Int J Infect Dis. 2020; 100:112–116. https://doi.org/10.1016/j.ijid.2020.08.076 PMID: 32891737

9. Cohen JI, Burbelo PD. Reinfection with SARS-CoV-2: Implications for Vaccines. Clin Infect Dis. 2020. https://doi.org/10.1093/cid/ciaa1866 PMID: 33338197

10. Tu YF, Chien CS, Yarmishyn AA, Lin YY, Luo YH, Lin YT, et al. A review of SARS-CoV-2 and the ongoing clinical trials. Int J Mol Sci. 2020; 21(7):2657. https://doi.org/10.3390/ijms21072657 PMID: 32290293

11. Jackson LA, Anderson EJ, Rouphael NG, Roberts PC, Makhene M, Coler RN, et al. An mRNA Vaccine against SARS-CoV-2—Preliminary Report. N Engl J Med. 2020; 383(20):1920–1931. https://doi.org/10.1056/NEJMoa2022483 PMID: 32663912

12. Mulligan MJ, Lyke KE, Kitchin N, Absalon J, Gurtman A, Lockhart S, et al. Phase I/II study of COVID-19 RNA vaccine BNT162b1 in adults. Nature. 2020; 586(7830):589–593. https://doi.org/10.1038/s41586-020-2639-4 PMID: 32785213

13. Zhou G, Zhao Q. Perspectives on therapeutic neutralizing antibodies against the Novel Coronavirus SARS-CoV-2. Int J Biol Sci. 2020; 16(10):1718–1723. https://doi.org/10.7150/ijbs.45123 PMID: 32226289

14. Gordon CJ, Tchesnokov EP, Woolner E, Perry JK, Feng JY, Porter DP, et al. Remdesivir is a direct-acting antiviral that inhibits RNA-dependent RNA polymerase from severe acute respiratory syndrome coronavirus 2 with high potency. J Biol Chem. 2020; 295(20):6785–6797. https://doi.org/10.1074/jbc.RA120.013679 PMID: 32284326

15. Wang Y, Zhang D, Du G, Du R, Zhao J, Jin Y, et al. Remdesivir in adults with severe COVID-19: a randomised, double-blind, placebo-controlled, multicentre trial. Lancet. 2020; 395(10236):1569–1578. https://doi.org/10.1016/S0140-6736(20)31022-9 PMID: 32423584

16. Goldman JD, Lye DCB, Hui DS, Marks KM, Bruno R, Montejano R, et al. Remdesivir for 5 or 10 Days in Patients with Severe Covid-19. N Engl J Med. 2020; 383(19):1827–1837. https://doi.org/10.1056/NEJMoa2015301 PMID: 32459919

17. McCallum M, De Marco A, Lempp F, Tortorici MA, Pinto D, Walls AC, et al. N-terminal domain antigenic mapping reveals a site of vulnerability for SARS-CoV-2. bioRxiv 2021.01.14.426475. Available from: https://www.biorxiv.org/content/10.1101/2021.01.14.426475v1

18. Wang Z, Schmidt F, Weisblum Y, Muecksch F, Barnes CO, Finkin S, et al. mRNA vaccine-elicited antibodies to SARS-CoV-2 and circulating variants. Nature. 2021.

19. Hoffmann M, Mösbauer K, Hofmann-Winkler H, Kaul A, Kleine-Weber H, Krüger N, et al. Chloroquine does not inhibit infection of human lung cells with SARS-CoV-2. Nature. 2020; 585(7826):588–590. https://doi.org/10.1038/s41586-020-2575-3 PMID: 32698190

20. Boulware DR, Pullen MF, Bangdiwala AS, Pastick KA, Lofgren SM, Okafor EC, et al. A Randomized Trial of Hydroxychloroquine as Postexposure Prophylaxis for Covid-19. N Engl J Med. 2020; 383(6):517–525. https://doi.org/10.1056/NEJMoa2016638 PMID: 32492293

21. Ogando NS, Dalebout TJ, Zevenhoven-Dobbe JC, Limpens RWAL, van der Meer Y, Caly L, et al. SARS-coronavirus-2 replication in Vero E6 cells: replication kinetics, rapid adaptation and cytopathology. J Gen Virol. 2020; 101:925–940. https://doi.org/10.1099/jgv.0.001453 PMID: 32568027

22. Sasaki M, Uemura K, Sato A, Toba S, Sanaki T, Maenaka K, et al. SARS-CoV-2 variants with mutations at the S1/S2 cleavage site are generated in vitro during propagation in TMPRSS2-deficient cells. PLoS Pathog. 2021; 17(1):e1009233. https://doi.org/10.1371/journal.ppat.1009233 PMID: 33476327

23. Chaudhry MZ, Eschke K, Grashoff M, Abassi L, Kim Y, Brunotte L, et al. SARS-CoV-2 Quasispecies Mediate Rapid Virus Evolution and Adaptation. bioRxiv 2020.08.10.241414. Available from: https://www.biorxiv.org/content/10.1101/2020.08.10.241414v1

24. Quentmeier H, Pommerenke C, Dirks WG, Eberth S, Koeppel M, MacLeod RAF, et al. The LL-100 panel: 100 cell lines for blood cancer studies. Sci Rep. 2019; 9(1):8218. https://doi.org/10.1038/s41598-019-44491-x PMID: 31160637

25. MacLeod RA, Nagel S, Scherr M, Pommerenke C, Koeppel M, Meyer C, et al. Human leukemia and lymphoma cell lines as models and resources. Curr Med Chem. 2008; 15(4):339–359. https://doi.org/10.2174/092986708783497319 PMID: 18288989

26. Hoffmann M, Kleine-Weber H, Schroeder S, Krüger N, Herrler T, Erichsen S, et al. SARS-CoV-2 cell entry depends on ACE2 and TMPRSS2 and is blocked by a clinically proven protease inhibitor. Cell. 2020; 181(2):271–280. https://doi.org/10.1016/j.cell.2020.02.052 PMID: 32142651

27. Walls AC, Park YJ, Tortorici MA, Wall A, McGuire AT, Veesler D. Structure, function, and antigenicity of the SARS-CoV-2 spike glycoprotein. Cell. 2020; 181(2):281–292. https://doi.org/10.1016/j.cell.2020.02.058 PMID: 32155444

28. Sheahan TP, Sims AC, Zhou S, Graham RL, Pruijssers AJ, Agostini ML, et al. An orally bioavailable broad-spectrum antiviral inhibits SARS-CoV-2 in human airway epithelial cell cultures and multiple coronaviruses in mice. Sci Transl Med. 2020; 12(541):eabb5883. https://doi.org/10.1126/scitranslmed.abb5883 PMID: 32253226

29. Lukassen S, Chua RL, Trefzer T, Kahn NC, Schneider MA, Muley T, et al. SARS-CoV-2 receptor ACE2 and TMPRSS2 are primarily expressed in bronchial transient secretory cells. EMBO J. 2020; 39(10): e105114. https://doi.org/10.15252/embj.20105114 PMID: 32246845

30. Zou X, Chen K, Zou J, Han P, Hao J, Han Z. Single-cell RNA-seq data analysis on the receptor ACE2 expression reveals the potential risk of different human organs vulnerable to 2019-nCoV infection. Front Med. 2020; 10(2):185–192. https://doi.org/10.1007/s11684-020-0754-0 PMID: 32170560

31. Qi F, Qian S, Zhang S, Zhang Z. Single cell RNA sequencing of 13 human tissues identify cell types and receptors of human coronaviruses. Biochem Biophys Res Commun. 2020; 526(1):135–140. https://doi.org/10.1016/j.bbrc.2020.03.044 PMID: 32199615

32. Cao Y, Liu X, Xiong L, Cai K. Imaging and clinical features of patients with 2019 novel coronavirus SARS-CoV-2: A systematic review and meta-analysis. J Med Virol. 2020; 92(9):1449–1459. https://doi.org/10.1002/jmv.25822 PMID: 32242947

33. Lamers MM, Beumer J, van der Vaart J, Knoops K, Puschhof J, Breugem TI, et al. SARS-CoV-2 productively infects human gut enterocytes. Science. 2020; 369(6499):50–54. https://doi.org/10.1126/science.abc1669 PMID: 32358202

34. Shulla A, Heald-Sargent T, Subramanya G, Zhao J, Perlman S, Gallagher T. A transmembrane serine protease is linked to the severe acute respiratory syndrome coronavirus receptor and activates virus entry. J Virol. 2011; 85(2):873–882. https://doi.org/10.1128/JVI.02062-10 PMID: 21068237

35. Zhou P, Yang XL, Wang XG, Hu B, Zhang L, Zhang W, et al. A pneumonia outbreak associated with a new coronavirus of probable bat origin. Nature. 2020; 579(7798):270–273. https://doi.org/10.1038/s41586-020-2012-7 PMID: 32015507

36. Wang P, Luo R, Zhang M, Wang Y, Song T, Tao T, et al. A cross-talk between epithelium and endothelium mediates human alveolar–capillary injury during SARS-CoV-2 infection. Cell Death Dis. 2020; 11(12):1042. https://doi.org/10.1038/s41419-020-03252-9 PMID: 33293527

37. Barretina J, Caponigro G, Stransky N, Venkatesan K, Margolin AA, Kim S, et al. The Cancer Cell Line Encyclopedia enables predictive modelling of anticancer drug sensitivity. Nature. 2012; 483(7391):603–607. https://doi.org/10.1038/nature11003 PMID: 22460905

38. Li W, Moore MJ, Vasilieva N, Sui J, Wong SK, Berne MA, et al. Angiotensin-converting enzyme 2 is a functional receptor for the SARS coronavirus. Nature. 2003; 426:450–454. https://doi.org/10.1038/nature02145 PMID: 14647384

39. Belouzard S, Chu VC, Whittaker GR. Activation of the SARS coronavirus spike protein via sequential proteolytic cleavage at two distinct sites. Proc Natl Acad Sci USA. 2009; 106(14):5871–5876. https://doi.org/10.1073/pnas.0809524106 PMID: 19321428

40. Zou L, Ruan F, Huang M, Liang L, Huang H, Hong Z, et al. SARS-CoV-2 viral load in upper respiratory specimens of infected patients. N Engl J Med. 2020; 382(12):1177–1179. https://doi.org/10.1056/NEJMc2001737 PMID: 32074444

41. Daly JL, Simonetti B, Klein K, Chen KE, Williamson MK, Antón-Plágaro C, et al. Neuropilin-1 is a host factor for SARS-CoV-2 infection. Science. 2020; 370:861–865. https://doi.org/10.1126/science.abd3072 PMID: 33082294

42. Cantuti-Castelvetri L, Ojha R, Pedro LD, Djannatian M, Franz J, Kuivanen S, et al. Neuropilin-1 facilitates SARS-CoV-2 cell entry and infectivity. Science. 2020; 370:856–860. https://doi.org/10.1126/science.abd2985 PMID: 33082293

43. Puelles VG, Lütgehetmann M, Lindenmeyer MT, Sperhake JP, Wong MN, Allweiss L, et al. Multiorgan and renal tropism of SARS-CoV-2. N Engl J Med. 2020; 383(6):590–592. https://doi.org/10.1056/NEJMc2011400 PMID: 32402155

44. Sungnak W, Huang N, Bécavin C, Berg M, Queen R, Litvinukova M, et al. SARS-CoV-2 entry factors are highly expressed in nasal epithelial cells together with innate immune genes. Nat Med. 2020; 26 (5):681–687. https://doi.org/10.1038/s41591-020-0868-6 PMID: 32327758

45. Singh M, Bansal V, Feschotte C. A Single-Cell RNA Expression Map of Human Coronavirus Entry Factors. Cell Rep. 2020; 32:108175. https://doi.org/10.1016/j.celrep.2020.108175 PMID: 32946807

46. Cheung KS, Hung IF, Chan PP, Lung KC, Tso E, Liu R, et al. Gastrointestinal manifestations of SARS-CoV-2 infection and virus load in fecal samples from the Hong Kong cohort and systematic review and meta-analysis. Gastroenterology. 2020; 159(1):81–95. https://doi.org/10.1053/j.gastro.2020.03.065 PMID: 32251668

47. Bojkova D, McGreig JE, McLaughlin KM, Masterson SG, Widera M, Krähling V, et el. SARS-CoV-2 and SARS-CoV differ in their cell tropism and drug sensitivity profiles. bioRxiv, 2020.04.03.024257. Available from: https://www.biorxiv.org/content/10.1101/2020.04.03.024257v1

48. Bertoglio F, Fühner V, Ruschig M, Heine PA, Abasi L, Klünemann T, et al. A SARS-CoV-2 neutralizing antibody selected from COVID-19 patients by phage display is binding to the ACE2-RBD interface and is tolerant to most known recently emerging RBD mutations. bioRxiv 2020.12.03.409318. Available from https://www.biorxiv.org/content/10.1101/2020.12.03.409318v2

49. Ng KW, Attig J, Bolland W, Young GR, Major J, Wrobel AG, et al. Tissue-specific and interferon-inducible expression of nonfunctional ACE2 through endogenous retroelement co-option. Nat Genet. 2020; 52(12):1294–1302. https://doi.org/10.1038/s41588-020-00732-8 PMID: 33077915

50. Onabajo OO, Banday AR, Stanifer ML, Yan W, Obajemu A, Santer DM, et al. Interferons and viruses induce a novel truncated ACE2 isoform and not the full-length SARS-CoV-2 receptor. Nat Genet. 2020; 52(12):1283–1293. https://doi.org/10.1038/s41588-020-00731-9 PMID: 33077916

51. Rehman SU, Tabish M. Alternative splicing of ACE2 possibly generates variants that may limit the entry of SARS-CoV-2: a potential therapeutic approach using SSOs. Clin Sci. 2020; 134:1143–1150. https://doi.org/10.1042/CS20200419 PMID: 32442315

52. Hou Y, Zhao J, Martin W, Kallianpur A, Chung MK, Jehi L, et al. New insights into genetic susceptibility of COVID-19: an ACE2 and TMPRSS2 polymorphism analysis. BMC Med. 2020; 18:216. https://doi.org/10.1186/s12916-020-01673-z PMID: 32664879

53. Howley PM, Knipe, David M. Fields Virology: Emerging Viruses. Wolters Kluwer Health; 2020. ISBN 978-1-975112-55-4

54. Wei J, Alfajaro MM, DeWeirdt PC, Hanna RE, Lu-Culligan WJ, Cai WL, et al. Genome-wide CRISPR Screens Reveal Host Factors Critical for SARS-CoV-2 Infection. Cell. 2021; 184(1):76–91. https://doi.org/10.1016/j.cell.2020.10.028 PMID: 33147444

55. Ou X, Liu Y, Lei X, Li P, Mi D, Ren L, et al. Characterization of spike glycoprotein of SARS-CoV-2 on virus entry and its immune cross-reactivity with SARS-CoV. Nat Commun. 2020; 11(1):1620. https://doi.org/10.1038/s41467-020-15562-9 PMID: 32221306

56. Wang K, Chen W, Zhang Z, Deng Y, Lian JQ, Du P, et al. CD147-spike protein is a novel route for SARS-CoV-2 infection to host cells. Signal Transduct Target Ther. 2020; 5(1):283. https://doi.org/10.1038/s41392-020-00426-x PMID: 33277466

57. Ziegler CGK, Allon SJ, Nyquist SK, Mbano IM, Miao VN, Tzouanas CN, et al. HCA Lung Biological Network. SARS-CoV-2 Receptor ACE2 Is an Interferon-Stimulated Gene in Human Airway Epithelial Cells and Is Detected in Specific Cell Subsets across Tissues. Cell. 2020; 181(5):1016–1035. https://doi.org/10.1016/j.cell.2020.04.035 PMID: 32413319

58. Smith JC, Sausville EL, Girish V, Yuan ML, Vasudevan A, John KM, et al. Cigarette smoke exposure and inflammatory signaling increase the expression of the SARS-CoV-2 receptor ACE2 in the respiratory tract. Dev Cell. 2020; 53(5):514–529. https://doi.org/10.1016/j.devcel.2020.05.012 PMID: 32425701

59. Uphoff CC, Pommerenke C, Denkmann SA, Drexler HG. Screening human cell lines for viral infections applying RNA-Seq data analysis. PLoS One. 2019; 14(1):e0210404. https://doi.org/10.1371/journal.pone.0210404 PMID: 30629668

60. Robinson JT, Thorvaldsdóttir H, Wenger AM, Zehir A, Mesirov JP. Variant review with the integrative genomics iewer. Cancer Res. 2017; 77(21):e31–e34. https://doi.org/10.1158/0008-5472.CAN-17-0337 PMID: 29092934

61. McKenna A, Hanna M, Banks E, Sivachenko A, Cibulskis K, Kernytsky A., et al. The genome analysis toolkit: a MapReduce framework for analyzing next-generation DNA sequencing data. Genome Res. 2010; 20:1297–1303. https://doi.org/10.1101/gr.107524.110 PMID: 20644199

62. McLaren W, Pritchard B, Rios D, Chen Y, Flicek P, Cunningham F. Deriving the consequences of genomic variants with the Ensembl API and SNP effect predictor. Bioinformatics. 2010; 26:2069–2070. https://doi.org/10.1093/bioinformatics/btq330 PMID: 20562413

63. Uphoff CC, Drexler HG. Comparative PCR analysis for detection of mycoplasma infections in continuous cell lines. In Vitro Cell Dev Biol Anim. 2002; 38:79–85. PMID: 11928999

64. Dirks WG, Drexler HG. STR DNA typing of human cell lines: detection of intra- and interspecies cross-contamination. Methods Mol Biol. 2013; 946:27–38. https://doi.org/10.1007/978-1-62703-128-8_3 PMID: 23179824

65. Corman VM, Landt O, Kaiser M, Molenkamp R, Meijer A, Chu DKW, et al. Detection of 2019 novel coronavirus (2019-nCoV) by real-time RT-PCR. Euro Surveill. 2020; 25:2000045. https://doi.org/10.2807/1560-7917.ES.2020.25.3.2000045

66. Quentmeier H, Schneider B, Röhrs S, Romani J, Zaborski M, Macleod RA, et al. SET-NUP214 fusion in acute myeloid leukemia—and T-cell acute lymphoblastic leukemia-derived cell lines. J Hematol Oncol. 2009; 2:3. https://doi.org/10.1186/1756-8722-2-3 PMID: 19166587